

IS THERE CHAOS IN THE ELECTRON MICROSCOPE?

D.Kunstelj

*Department of Physics, Faculty of Science (PMF), University of Zagreb,
Bijenička c.32,10000 Zagreb, Croatia*

M.Martinis and A.Knežević

"Rudjer Bošković" Institute, Bijenička c. 54,10000 Zagreb, Croatia

Abstract

High-temperature superconductor $Bi_2Sr_2CaCu_2O_8 + x$ has been investigated by the high-resolution electron microscope (HREM) and the photodensitometric technique in order to resolve the sub-atomic shifts in the modulated structure. This investigation has shown that the background noise is pronounced, indicating some kind of ordering in certain crystallographic directions. We have found that the "mapping" of the charge densities by the inverse Fourier transform of the diffracted electron image and the connections to the crystal structure can be easily established in the case of elastically, as well as the inelastically scattered electrons. The order of the details in so obtained "inelastic" electron "micrographs", as well as the dependence of the structure of the EM image on the initial conditions of the inverse Fourier transform, leads to the conclusion that there is an order emerging from the diffuse scattered electron diffraction patterns. Data sets from digitalized densitograms are analysed by the Rescaled range (R/S) method in order to study fractal and long-range correlation properties of the inelastic scattered electrons in the "noise" region between Bragg reflections. The results of the R/S analysis showed that the value of the Hurst exponent was $H \neq 0.5$, indicating that the "ordering" of the noise in the Inverse (Fourier) space was much more pronounced at longer distances (about 440 atom spacings), then for shorter distances of about 55 atom spacings.

1 Introduction

Electron micrographs of high resolution (HREM) show an considerable amount of the background noise superimposed on regularly arranged network of motifs representing the order in the crystal lattice. The background noise has various

origins. One is the inelastic interaction of incoming electrons with host electrons and phonons of the sample under investigation. The final image which is the convolution of these inelastic, and other effects will be disordered to some extent, showing general regular crystal motif smeared by diffuse scattered electrons. Now, we may ask the question: Are those diffusely scattered electrons really stochastically distributed in space as seen in Fig.1a,b and Fig.2b,c, or there is some kind of the order emerging from the interaction of the EM electrons with the charge distribution in the specimen? Is there really some regularity in the diffuse scattering of the EM electrons transmitting the sample ("diffuse background"). In other word, do we see some chaotic order in high resolution electron micrographs?

In order to study the contribution of the diffusely scattered electrons to the micrograph, we should be able to separate their effect from the effect of elastically scattered electrons on the intensity of the electron beams impinging the photographic plate in the electron microscope. For this purpose we process the EM micrograph following the events of the image formation in the microscope. Apart from the modulation of the EM electron intensities by the instrument itself (transfer function) and the mode of the operation conditions applied in detection of the particular motif under investigation (focussing conditions), formation of the image consists of diffraction of the EM electrons, their interference and the amplitude reconstruction. This processes are well described by the Fourier transforms and may be simulated by a suitable computer program. So the EM image may be processed following the events in the electron microscope. The computer program should be able to separate elastically as well as inelastically diffracted "electron beams" which contribute to the formation of the image. One of them is ProFFT (Professional Fast Fourier Transform), which enables us to explore the Brillouin zones of the crystal one by one, their sections, and to map the results of the interactions of the EM electrons with the charge densities of the host crystal.

2 Experimental

2.1 Basic electron microscopy of the $Bi_2Sr_2CaCu_2O_8 + x$ non-modulated samples

The figure of non-modulated structure of $Bi_2Sr_2CaCu_2O_8 + x$ high-temperature superconductor ($T_{sc} = 85$ K), obtained by HREM [1, Fig.2] was scanned and

entered to ProFFT program. This image (reproduced with the laser printer) shown in Fig.1a, resembles very well the original. White dots in the rectangular array represent dominantly the Bi atom columns, which are the strongest electron scatterers, the \mathbf{c} projection of the elemental cell is shown on the right side (**a,b**) of the figure. The laser aided optical Fourier transform (OFT) which was made using the EM micrograph negative [1], is shown in the same figure, with the main reflections labeled as the insert down left. The diffraction pattern of this figure, i.e., its Fourier transform is obtained by applying the ProFFT and presented in Fig.1b. The main reflections of the unit cell are labelled, the "filtering ring" and the "filtering cross" are shown as well. The "filtering ring" allows the diffusely scattered electrons with $\mathbf{k}(x')^2 + \mathbf{k}(y')^2 = \mathbf{k}(x', y')^2 = const.$ (x' and y' being the coordinates of the Inverse space), i.e. with a certain kinetic energy, to enter the next step, the Inverse Fast Fourier transform (IFFT), of the image formation. This way, we obtain the picture, or the map, of the diffuse scattered EM electrons which suffered a certain amount of the energy gain or loss when passing the sample. If we use "the cross filtering", we can choose any $\mathbf{k}(x')$ and/or $\mathbf{k}(y')$, their interval, or their linear combination in the inverse (Fourier) space ($\mathbf{k}(x') + \mathbf{k}(y') = \mathbf{k}(x', y')$), and to show the map of the energy losses, or gains, of the transmitting electrons in specific directions, and to see if this losses are Stochastic or Chaotic in their nature. Fig.2a,[1], shows nearly sinusoidal behaviour of the contrast along the rows a and b of the atoms (a), level fluctuations is caused by the uneven blackening of the negative of the EM photograph. The Fourier transform of the digitalized trace shown in Fig.2a is presented in Fig.2b, the peak corresponds to the (200) reflection, with the crystal plane spacings of 2.715 A.U. The same was done for the b direction, and the result is shown in Fig.2c. To the left (I. and the II. Brillouin zones.) and to the right (higher Brillouin zones.) of labelled Bragg reflections, the photodensitometric trace of the diffuse background shows no distinctive regularities, and, at this step of the observations may be described as purely stochastic, or nondeterministic. Subsidiary maxima close to the (020) reflection in Fig.2c, may be due to the initialization of some crystal ordering [1], this matter is elaborated in Ref.1, and is beyond the scope of the present paper.

Now, we can do the procedure as described above, i.e., to select a certain combination of $\mathbf{k}(x')$ and $\mathbf{k}(y')$, to make an IFFT procedure, and to compare the density map so obtained with the crystal structure. In order to check the whole procedure the crystal structure itself was "purified" by blocking the background between the Bragg reflections, once (Fig.3a) and repeating the procedure, i.e.,

twice (Fig.3b). It can be seen that the contrast and the informations about the details of the figure are augmented this way. This is much better shown in Fig.4a (enlarged detail of Fig.1a), and 4b (enlarged detail of Fig.3b), where, for the precise measurements of the charge density positions, the sketch of the crystal lattice is superimposed upon the EM image (White arrows on the left are the orientation marks). It is well seen that the main charge densities, i.e., the positions of atoms (atom columns) are centered at the crystal lattice nodes, the lattice parameters in the a and b directions are nearly the same, being about 5.4 A.U.[1]. So, this figure, which we interpret as the projection of the charge densities of the crystal lattice, can serve as the standard for the further investigations.

2.2 Experimental situation and some theoretical considerations

First we do short overlook of the experimental situation in our case, and then some theoretical considerations and approximate calculations. Let us see what is going on with the 200 keV electrons when passing through the crystalline sample, 10 to 20 nm thick, at the approximate temperature of about 400 K, with the relativistic speed of about 2/3 of the speed of light. They "see" the crystal lattice, which vibrates according to $k_B T = hf$, with the frequency of the order of 10^{13} Hz, k_B being the Boltzmann constant, and h the Planck constant. The "time of flight" of the 200 keV electron through the sample of about 10 nm is simply then about half of 10^{-16} seconds, which is 5/10000 of the estimated period of the period of atom vibrations. So the every wavefront of the EM electrons see "frozen" lattice, but, each incoming wavefront in a different state of the lattice vibrations, longitudinal and transversal. As the exposure of an EM negative takes one to two seconds, we get the picture of about $n = t(exposure)/t(flight) = 4 \cdot 10^{16}$ slightly different states of the atom positions, vibrating inside the "volume" of an atom, with the phonon spectrum given by the crystal lattice and its atoms, being at the temperature of about 400 K. So the EM electrons "see" the phonon spectrum of the sample, that is all vibration states, and "transfer" it to the EM negative. The ergodicity of the system is thus fulfilled, and so the Liouville's theorem holds.

The average positions of the atoms thus give spread (Debye-Waller broadening) Bragg reflections, i.e., the Fourier transform of the lattice. The inelastic interactions of the EM electrons with phonons may give what we usually call the

background noise, which may be of the chaotic nature, that is, with some order dictated by the phonon spectrum and the host electron states. The next event is the interaction of the EM electrons with the host electrons; that bounded within the inner electronic shells of the atoms, the valency electrons, and the loosely bonded "wandering", i.e. conduction electrons. The interactions of the EM electrons with the inner shells (K,L,M,...), with the energy exchange of the order of keV-s, shall not be considered here, because this matter is covered by the very well known EELS (Electron Energy Loss Spectroscopy), and the diffracted inelastically scattered electrons lie far away the usually recorded diffraction pattern, that is, far from the origin of the Fourier transform of the observed crystal lattice. Now, let us see what we can really do by making some short and simplified calculations of the inelastic interactions of the EM electrons and the loosely bounded electrons in our sample. The energy loss calculation may be simply argued by the observation of the background diffuse scattering within the 1st and the 2nd Brillouin zones in the diffraction pattern (Fourier transform) of the crystal (Fig.1a., insert down left, Fig.1b.), which is obtained by making the Fourier transform of the crystal lattice using the ProFFT (Professional Fast Fourier Transform) program. The calculations are based on the use of the Bragg equation, which is extended with the inelastic member, i.e., in the vector form this equation is now: $\mathbf{k} - \mathbf{k}_0 = \mathbf{g} + \mathbf{dk}$; within the 1st and the 2nd Brillouin zones $\mathbf{g} = \mathbf{0}$, and the \mathbf{dk} is the inelastic member which can be calculated from its position in the 1st and the 2nd Brillouin zones using the diffraction pattern as follows. Let dk coming from the the energy loss being exactly at the half of the (200) position, that is at the edge of the 1st Brillouin zone (1st.B.z.) in the [100] direction. Then $dk = g/2 = 1/2d(200)$; with $d(200)$ in our case being $2,715 \text{ \AA} = 2,7 \cdot 10^{-10} \text{ m}$, so $dk = 1,84 \cdot 10^9 \text{ m}^{-1}$. The energy loss we calculate from the expression for the kinetic energy of a free particle: $E = (hk)^2/2m$, $h=6,6236 \cdot 10^{-34} \text{ Js}$ is the Planck constant, $m=9,11 \cdot 10^{-31} \text{ kg}$, the mass of an electron, $k = dk$ for the edge of the 1st.B.z., so the energy loss $E = 8,15 \cdot 10^{-19} \text{ J} = 5 \text{ eV}$. The energy is proportional to k^2 , so the energy loss of an inelastically scattered electron at the edge of the 2nd.B.z. ($k_2 = 2k_1$) is of the order of 20 eV. So, by the simple selection of the part of the Inverse Space generated by the Fourier transform (Paragraph 1.) we can investigate the the electron energy loss spectra and the space distribution of inelastically scattered electrons in the range up to 20 eV by using the FFT and IFFT procedures of the ProFFT program as described above.

2.3 The Rescaled Range (R/S) analysis of the "noise" in the densitograms of the High Resolution Electron micrographs

Data sets of 512 (2^9) points (about 55 atom spacings) are cut from the whole of 4096 (2^{12}) points (about 440 atom spacings), from digitalized densitograms [1] of ten different traces along a[200] and b[020] directions of the BISCO ($\text{Bi}_2\text{Sr}_2\text{CaCu}_2\text{O}_{8+x}$) crystal, in order to analyse the existence of short/ or long range correlations in the "noise" region between Bragg reflections. An example of densitogram [1] is shown in Fig.2a.

As we believe that such "noise" arises from interactions of incoming electron beam with crystal lattice, such as electron-phonon and electron-electron inelastic scatterings, it could bring some informations from the system. In terms of nonlinear analysis we expect for signals to have a long-range correlation properties and not be white noise (complete random data).

The Rescaled range (R/S) method of nonlinear analysis was used to study the correlation properties in our data sets [2,3,4]. The method is related to the evaluation of the Hurst scaling exponent, H. Different values of the Hurst exponents correspond to different correlation properties.

For the signal represented by the data set $u(n)$, $n = 1, \dots, N$ in one crystallographic direction we calculated the running average $\bar{u}(n)$ and the accumulated deviations from the average $X(l, n)$;

$$\bar{u}(n) = \frac{1}{n} \sum_{k=1}^n u(k)$$

$$X(l, n) = \sum_{k=1}^l [u(k) - \bar{u}(n)]$$

The quantity called the range $R(n)$ of $X(l, n)$ and the standard deviation $S(n)$ are defined as follows:

$$R(n) = \max_l X(l, n) - \min_l X(l, n)$$

$$S(n) = \sqrt{\frac{1}{n} \sum_{k=1}^n (u(k) - \bar{u}(n))^2}$$

The "rescaled range" is defined as a ratio between R and S (R/S). The power law scaling according to Hurst is:

$$R(n)/S(n) \sim n^H$$

where H is the Hurst exponent. If a signal represents white noise (uncorrelated signal) then $H=0.5$. If $H \neq 0.5$, the long-range correlations (memory) are in the system.

The scaling exponent H is evaluated from the $\log(R/S)$ vs. $\log(n)$ plot using the least square fit procedure.

The running procedure is as follows: we calculate R/S for one box of n points, starting with first two points. In the next step we add one point more and calculate R/S for the wider box and so on, until the box has length N of starting data set. In this way we always hold one box with fixed left and moving right end.

The results of the analysis are shown in Fig.5. This figure is the representative of 21 analysis worked on traces of the BISCO crystal lattice.

2.4 The ProFFT analysis of the diffuse scattering in HREM micrographs of BISCO

The evolution of an physical system is usually described in the 6D phase space, which is defined by 6 degrees of freedom; 3 space coordinates and 3 impulse coordinates (\mathbf{r}, \mathbf{p}). A priori all the states of the system are equally probable (Liouville's theorem) and the probability of the state of the system is equal to the time average of the ensemble (Ergodic theorem; ensemble may be one particle). The "volume" of the phase space is determined with the total energy of the system. The phase space can be "divided" (separated) into subspaces according to the specific problems of the system investigated. So, we may choose to represent the system in Cartesian coordinates ($\mathbf{r}(x,y,z)$), so called the Direct space; or/and we may use the impulse coordinates ($\mathbf{p}(p_x, p_y, p_z)$), so called the Inverse space. This two spaces are then connected with the Fourier transformations. The trajectories of the system which undergoes the chaotic behaviour in the 6D phase space are usually presented as its projections known as the Poincare sections, in order to get the 2D presentation in, say, (x, p_x) projection. We may also choose another coordinate subsystems of the 6D phase space to present our problem, so we can take the Direct space (charge distribution in the crystal) and the Inverse space (i.e. the diffraction pattern in the reciprocal space), which two are then connected by the Fourier transformations.

The Direct and the Inverse space are easy to explore experimentally by the use of the High Resolution Electron Microscopy (HREM), taking the image and the corresponding diffraction pattern of the crystal. The HREM data can be digitalized and further explored by the computer programs which are based on the use of the Fourier transforms (ProFFT). In this respect, following our R/S analysis (paragraph 2.3), we first explored the situations in x and y directions (HREM micrographs), and the $k_{x'}$ and $k_{y'}$ directions (the diffraction patterns). Here we concentrated on the diffuse scattered electrons in the 1st and 2nd Brillouin zones, that is from the origin up to (200) reflections (Fig.1b). If we take the horizontal part of the cross, which we obtain by proper masking of the whole diffraction pattern (the [020] and the opposite direction, down left insert in Fig.1b), and the use of ProFFT programm to perform the Fourier transformation, we obtain the situation as shown in Fig.6a. Analogously, taking the vertical part of the cross, which contain the diffuse scattered electrons in the [200] direction, to contribute to the image formation, we obtain the distribution of the diffuse scattered EM electrons with an energy loss, as shown in Fig.6b. In both figures, Fig.6a and b, we can recognize white bands ("stripes") on dark background and dark bands ("stripes") on the pale (white) background. The stripes are perpendicular to the direction of the analogous reflection in the diffraction pattern, they are approximately equidistant, and more or less "paired". They can also "merge" to each other, which is somewhat better seen in Fig. 6a. The white and the dark stripes are nearly of the distance as the atom columns in Fig.1a. So we can interpret them as the result of the inelastic scattering of the EM electrons at the atom sites, with the absorption of some energy (dark stripes on white bands), and the re-emission of similar energy (white stripes on the dark bands).

This figures do not say anything about the possible charge distribution and the inelastic scattering between the atom columns positions, which may be present if there is some charge transfer between the neighbouring atoms. To explore this possibility we may use the whole cross from Fig.1b, or the half of it, that is from the origin of the reciprocal space to the half distance to the (200) and the (020) maxima. This way we are taking only the inelastically scattered electrons with the energy losses in the 1st Brillouin zone. We can easily calculate this band of energies (The basis of this calculation is already given in 2.2.). Moreover, we can mask any part of the diffraction pattern, and by the use of the ProFFT, see the distribution of the diffusely scattered electrons with certain energy loss. (Here we emphasize the regularity of the order of the stripes show-

ing the regularity of the energy losses of diffusely scattered electrons, in relation to the diffuse background in the diffraction patterns (Fig.1, Fig.2b,c), which are "chaotic". This regularity may be explained with the quantization of the energy transfer between the EM electrons and the charge and phonons in the sample, as well as with the specific atom positions in the crystal lattice.) Thus, in Fig.7a and 7b we present the images of inelastically scattered electrons in the 1st and the 2nd B.zones superimposed on the crystal grid, which was taken from Fig.1a in order to correlate them to the positions of the atom columns (**a** and **b** are as in Fig.1a, white arrows on the left-down of the images in Fig.7a and 7b are reference marks.). The diffusely scattered electrons are positioned at the atom sites, i.e., on the crossings of superimposed crystal grid, and between them. The patches are "dark" on the white background, this shows the absorption in this directions, and "white" on dark background, which shows the diffraction in that direction. This "secondary" diffractions are probably due to the elastic diffraction of the EM electrons which were already subjected to energy loss by the inelastic scattering. This two possibilities are, for huge number of the EM electrons involved in the image formation, the same, so the number of "white" and "dark" patches is expected to be equal, as easily seen by the inspection of Fig.7. In addition, white (pale) and the dark (gray) "bridges" between inelastically scattered electron maxima we interpret as inelastic interactions with the valence electrons and the phonons in the **a** and the **b** directions, i.e. along the directions of the elemental cell. Also, it has to be noted that the diffusely scattered maxima ("white" as well as "dark") are equally positioned between the crystal nodes, which may be the result of a very different causes that has to be still more explored. For example, "white" as well as the "dark" patches may be the result of different, but quantized, energy losses which are close in the amount and the scattering direction. Or, they can be the result of the extended crystal defect, which is not recognized in the direct EM image (Fig.1a).

However, the regularity of the diffuse scattering is evident. This phenomenon is demonstrated by the experiment in which the initial conditions are slightly changed, i.e., the cross, which defines the number of inelastically scattered electrons which form the image, can be slightly changed, say by narrowing it, as was done for Fig.7b in comparison to Fig.7a. The general appearance of this figures is nearly the same, they only differ in details, for example in the intensity, but not the position of the "white" and the "dark" patches. This was to be expected, because the nature of the physical processes was not changed by this intervention, only the number of the inelastically scattered electrons which

form the image. This is the result of the chaotic behaviour of the system in the case we do not go far in change from the initial conditions, and if the Liapunov coefficient is not too big for the interval of the exposition time. Fig.7a and Fig.7b show that our presumptions are fulfilled.

In our investigations of the image formation in the Electron microscope by exploring the inelastically scattered electrons contribution we used a non-standard approach in the analysis of the chaotic nature of the system by observing the connections of the Direct and the Inverse space by applying the Fourier transformations. (Usually, the possible chaotic nature of the physical system is investigated by the analysis of the \mathbf{r}, \mathbf{p} -pairs projections of the Phase space (Poincare sections). Here, our "Poincare sections" of the Phase space are \mathbf{x} and \mathbf{y} coordinates in the Direct, crystal space, which are connected to the analogous \mathbf{p}_x and \mathbf{p}_y coordinates in the Inverse space by the Fourier transformations).

3 Disussion

We show that in the Direct space of the crystal there is a definite order of atoms (Fig.1a, Fig.2a, Fig.3a,b, Fig.4a,b). Also, the main result of our analysis of the inelastically (diffusely) scattered electrons (Fig.6 a,b, Fig.7a,b) is that there is the definite order in their diffraction, which was demonstrated by the use of the Fourier transform as described in the previous section. The independent R/S analysis (Fig.5) also showed that there is a long range order in, at the first sight stochastically chaotic background in the Inverse space (diffuse background in Fig.1b and Fig.2b,c). So we concluded that our process of the image formation in the Electron microscope is chaotic in its nature. The physical background of such conclusion is proposed in the paragraph 2.2 of the paper.

To illustrate this standpoint we enclose one more result of our investigations in Fig.8. The results presented in the previous paragraph and the considerations of the physical system we explored allow us to propose the model for the theoretical elaboration of the problem, which task is far from the matter here elaborated. First, the possibility of investigation of the influence of crystal oscillations on the electron-phonon energy exchange we see in connection to the very well known model of the situation known as The Fermi acceleration [5]. In this model, as shown in Fig. 8a, the particle (our EM electron) meets the potential, which oscillates with some amplitude (a) with a certain frequency. The amplitude and the frequency may be estimated from the Debye-Waller factor for the system under investigation, if the temperature of the sample is known. In

the next step this model may be connected to the Quantum billiard system [6], in which the billiard walls oscillate to produce the Fermi acceleration, thus simulating the oscillating crystal lattice. The result may be as in Fig.8b, in which a contours of the quantum mechanical wave function, whose classical counterpart has chaotic behaviour, are shown [6]. In this sketch of the wave function solid lines indicate positive values, and the dashed lines negative values, which may present the emission and the absorption of inelastically scattered electrons respectively. This figure may be connected with our observations, one example is shown in Fig.8c, where the "positive" parts are shown as white areas containing somewhat darker patches, and the "negative" parts are shown as dark areas with a pale patches; also presenting the absorption and re-emission processes, as proposed in the previous paragraph. Figure 8c was obtained by the same procedure as applied for Fig.7, but with electrons filtered by a ring (Fig.1b, insert up right), thus allowing the inelastically scattered electrons of approximately same energy, but in an energy band defined by the wideness of the ring, to enter the Fourier transform procedure (ProFFT), and to show the inelastically scattered electron density map.

The situation with "white" and "dark" patches is similar to that in Fig. 2.7. They are of approximately same size, distributed at approximately same distance, somewhere connected with the "bridges", but less than in Fig.7. Thus we conclude that the diffusely scattered electrons with approximately same lost or regained energy (Fig.8c) are more localized than diffusely scattered electrons within a wider energy band (1st and 2nd Brillouin zone, Fig.7), the result which was expected. The connections of the patches showing the positions of the diffusely scattered electrons may show the ways which may be used by the conduction electrons when conducting the electric current in the "normal" state and in the superconducting state as well.

ACKNOWLEDGEMENT

The authors acknowledge the use of the data from Ref.1. This work was supported by the Ministry of Science and Technology of Croatia under the contract 119203 and 0098004.

References

- [1] D. Kunstelj, D. Babić, D. Bagović, B. Leontić, Z. Vučić, and J. Gladić, phys.stat.sol.(a), No.2, 165(1998)p.467.

- [2] H. E. Hurst, Trans.Am.Soc.Civ.Eng. 116(1951)770.
- [3] J. Feder, Fractals, Plenum Press, New York, 1988.
- [4] H. E. Hurst, R. P. Black, Y. M. Simaika, Proc.(1991)3557.
- [5] H. J. Korsch, H.-J. Jodl, Chaos, Springer Verlag, Berlin-Heidelberg,1994.
- [6] R. C. Hilborn, Chaos and Nonlinear Dynamics, Oxford University Press, New York 1994.

FIGURE CAPTIONS

Fig.1 a) HREM image of $\text{Bi}_2\text{Sr}_2\text{CaCu}_2\text{O}_{8+x}$ high temperature superconductor, $T_c = 85\text{K}$. The insert down left is its optical (laser) diffraction pattern.

b) Fast Fourier Transform (FFT) of Fig.1a. Most of inelastically scattered electrons are inside two first Brillouin zones. Inserts up right and down left show the modes of analysis of Fig.1a when using inelastically scattered electrons (see text).

Fig.2 a) Photodensitometric trace of Fig.1a along $[200]$ direction. Similar trace is obtained along $[020]$ direction. These traces, digitalized, are used in the R/S analysis.

b) FFT of the trace shown in a). c)FFT of the trace in $[020]$ direction. The diffuse backgrounds inside (200) and (020) are analysed in present paper.

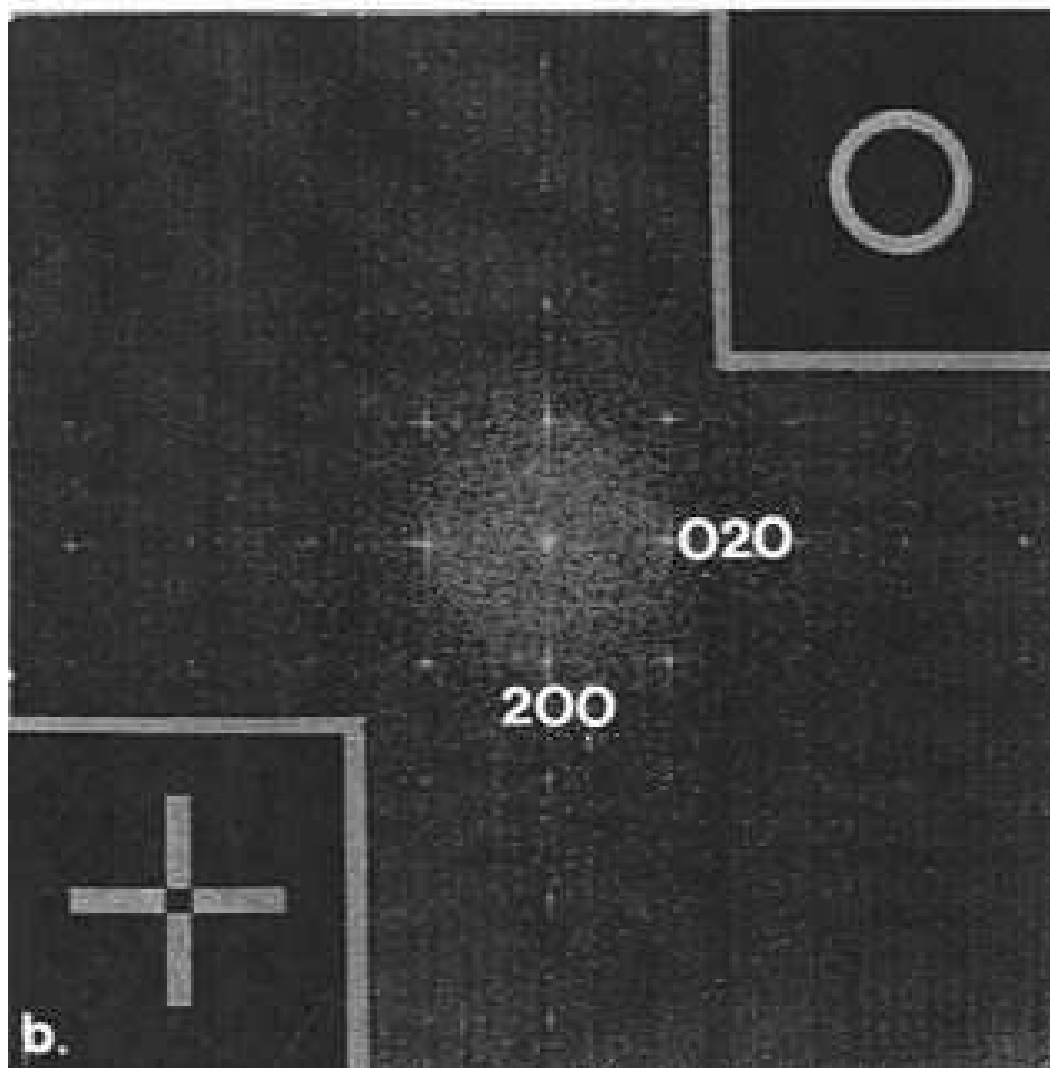
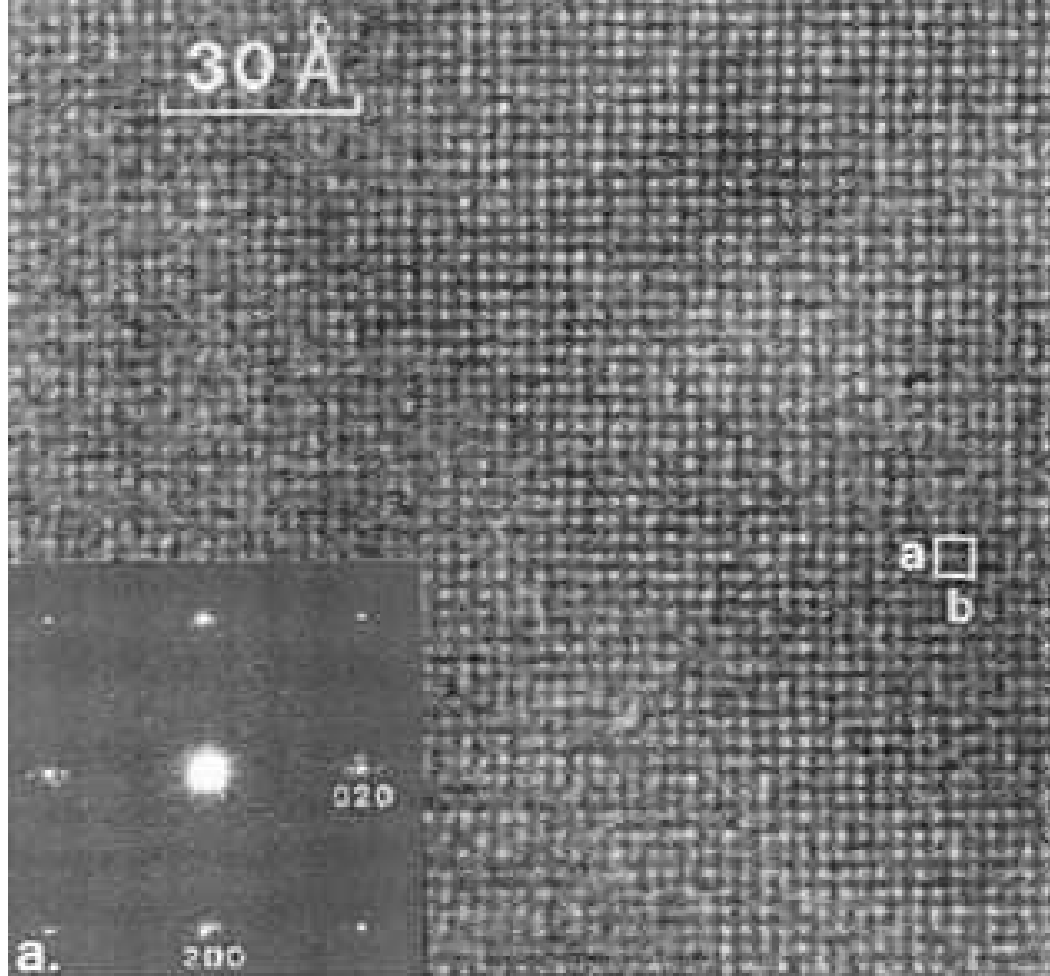
Fig.3 a) Filtered image of Fig.1a. The Bragg reflections used in the ProFFT programm are shown nonmasked in the insert up right. This figure shows up "clear" crystal lattice.

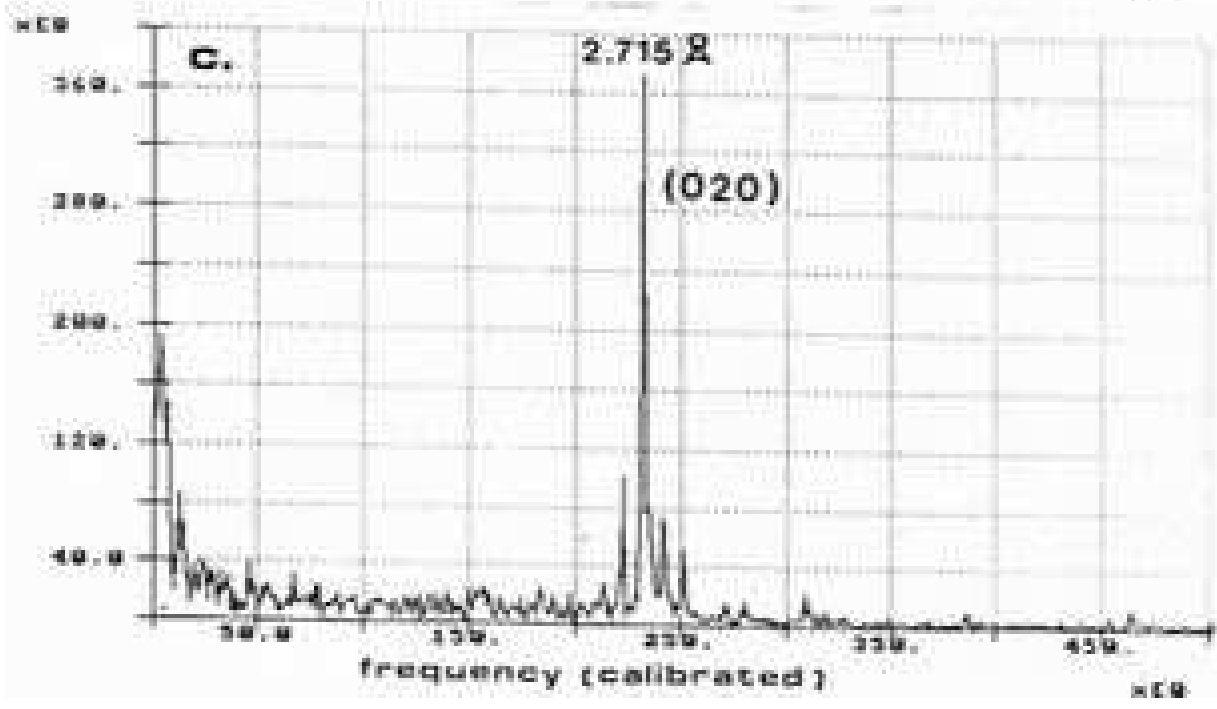
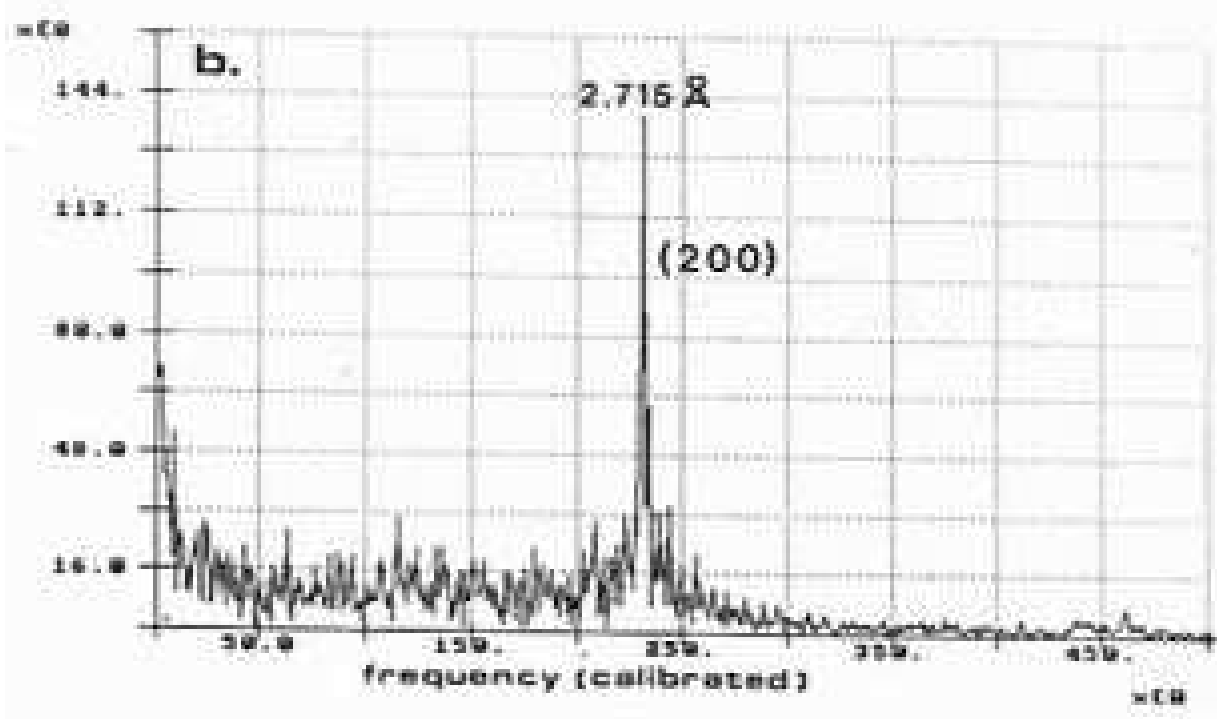
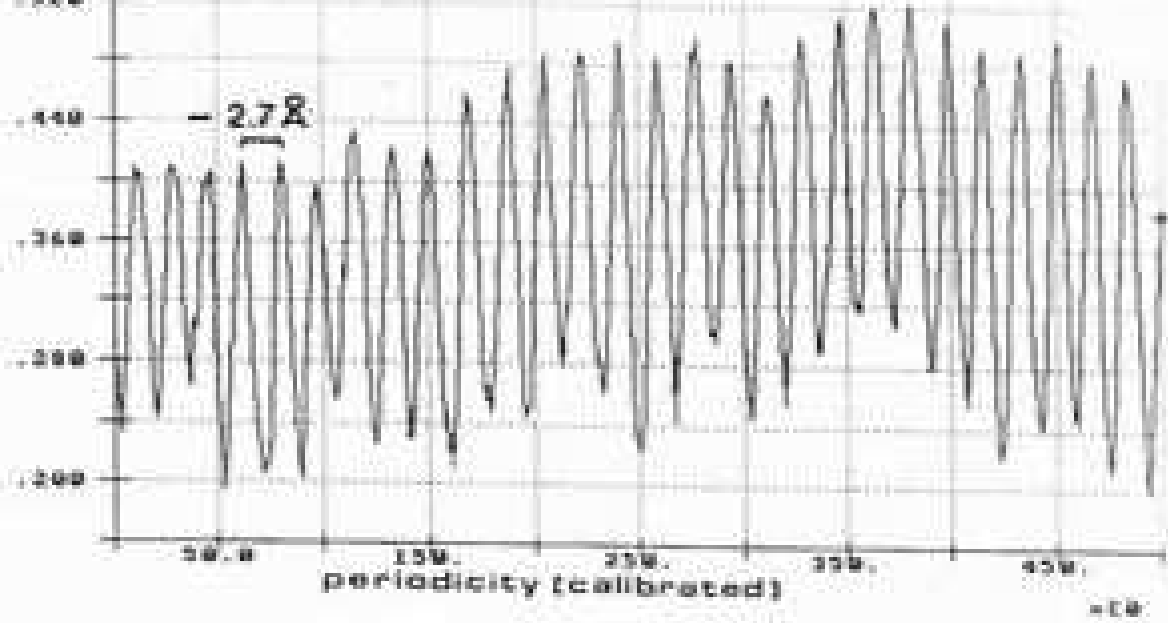
b) Double filtered image of the same detail of the crystal shown in Fig.1a. Fine mosaic substructure is now better emphasized. The appearance of faint reflections of the (110) type is not investigated here.

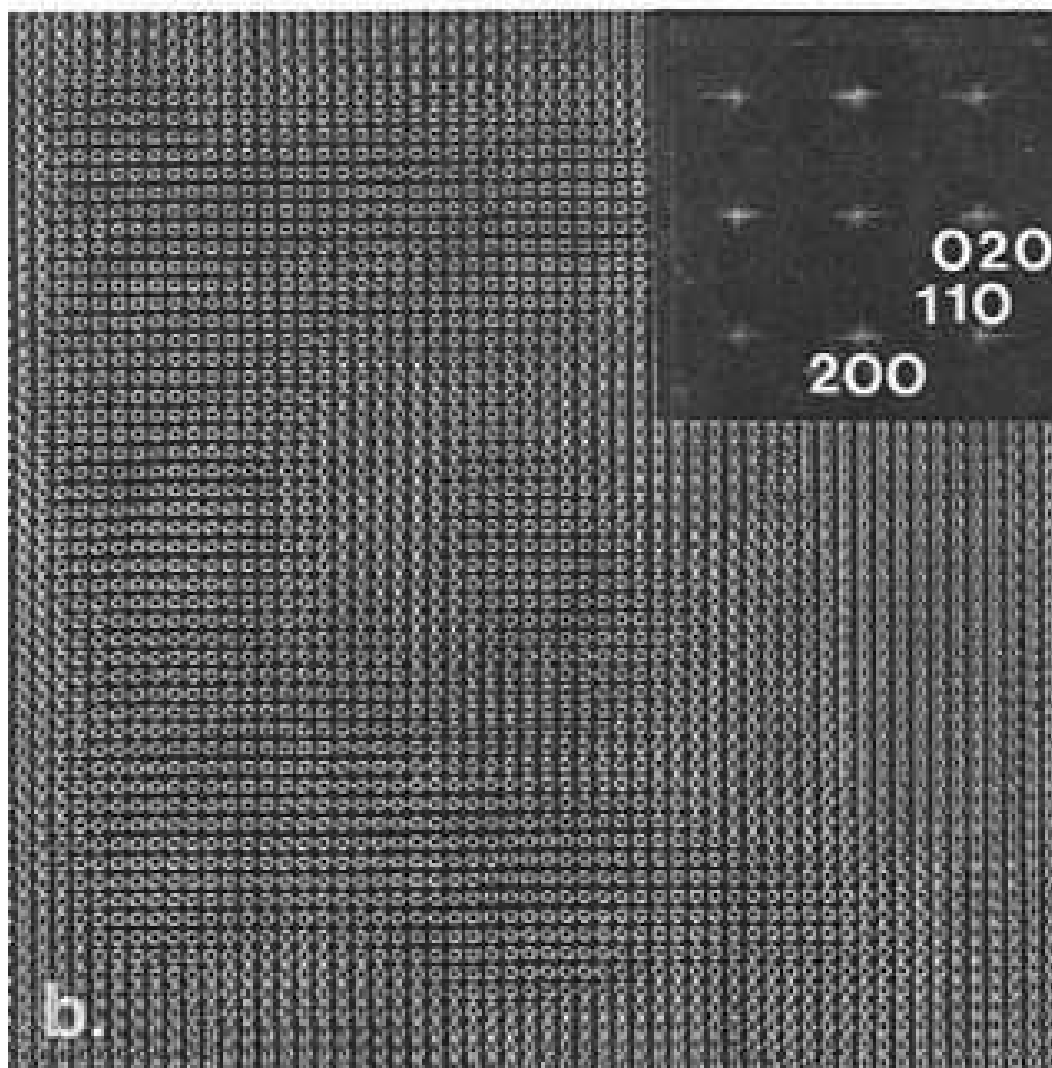
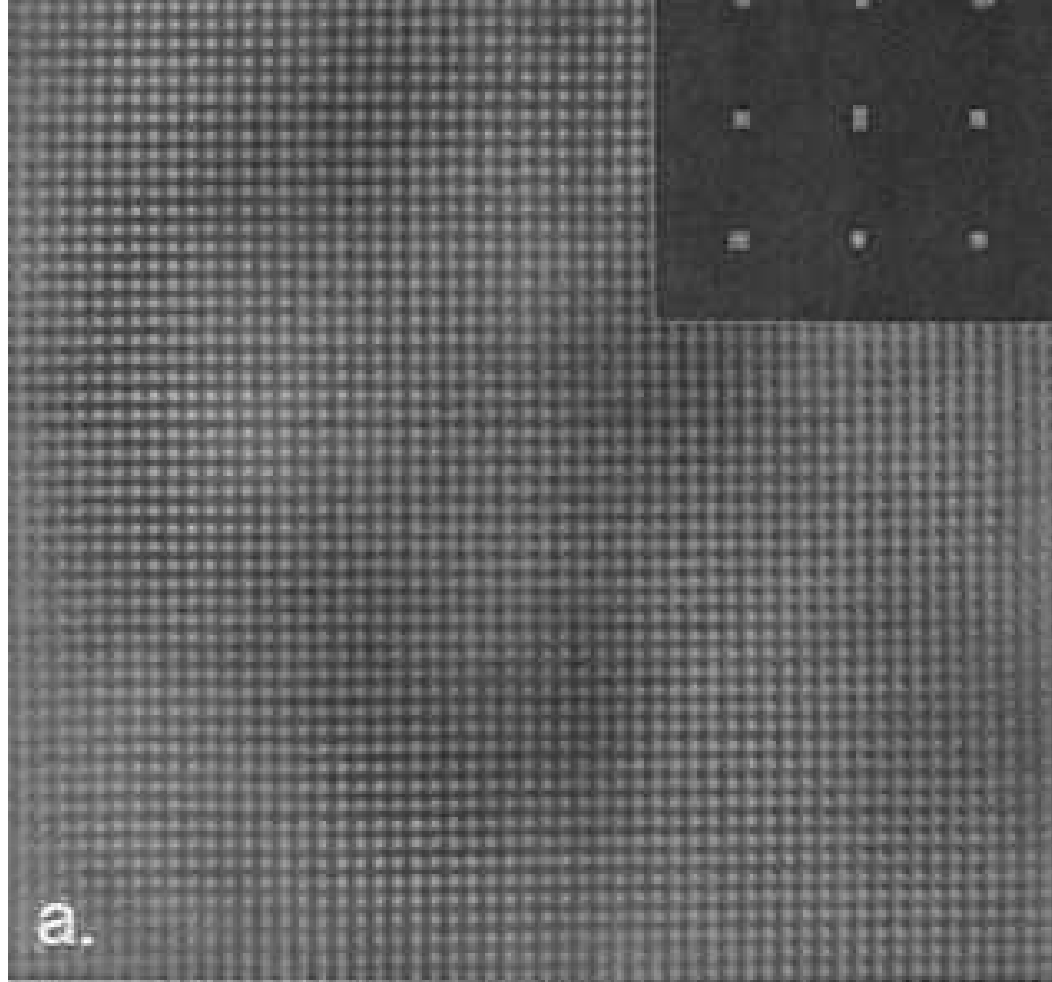
Fig.4 a) Fig.1a highly computer magnified and superimposed on the crystal grid with $a=b=5.4$ A.U. to show that the atom columns lie on the crystal nodes.

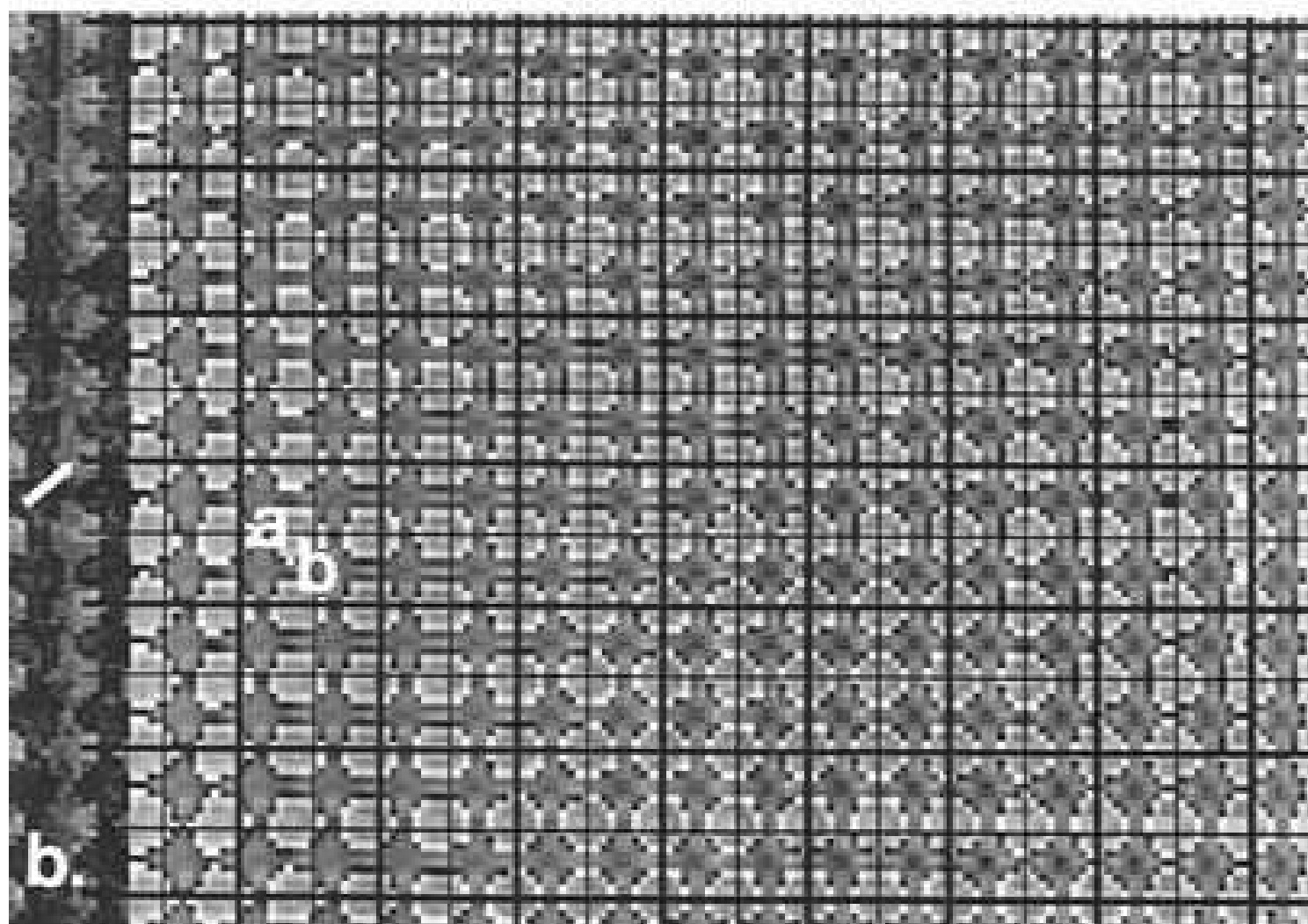
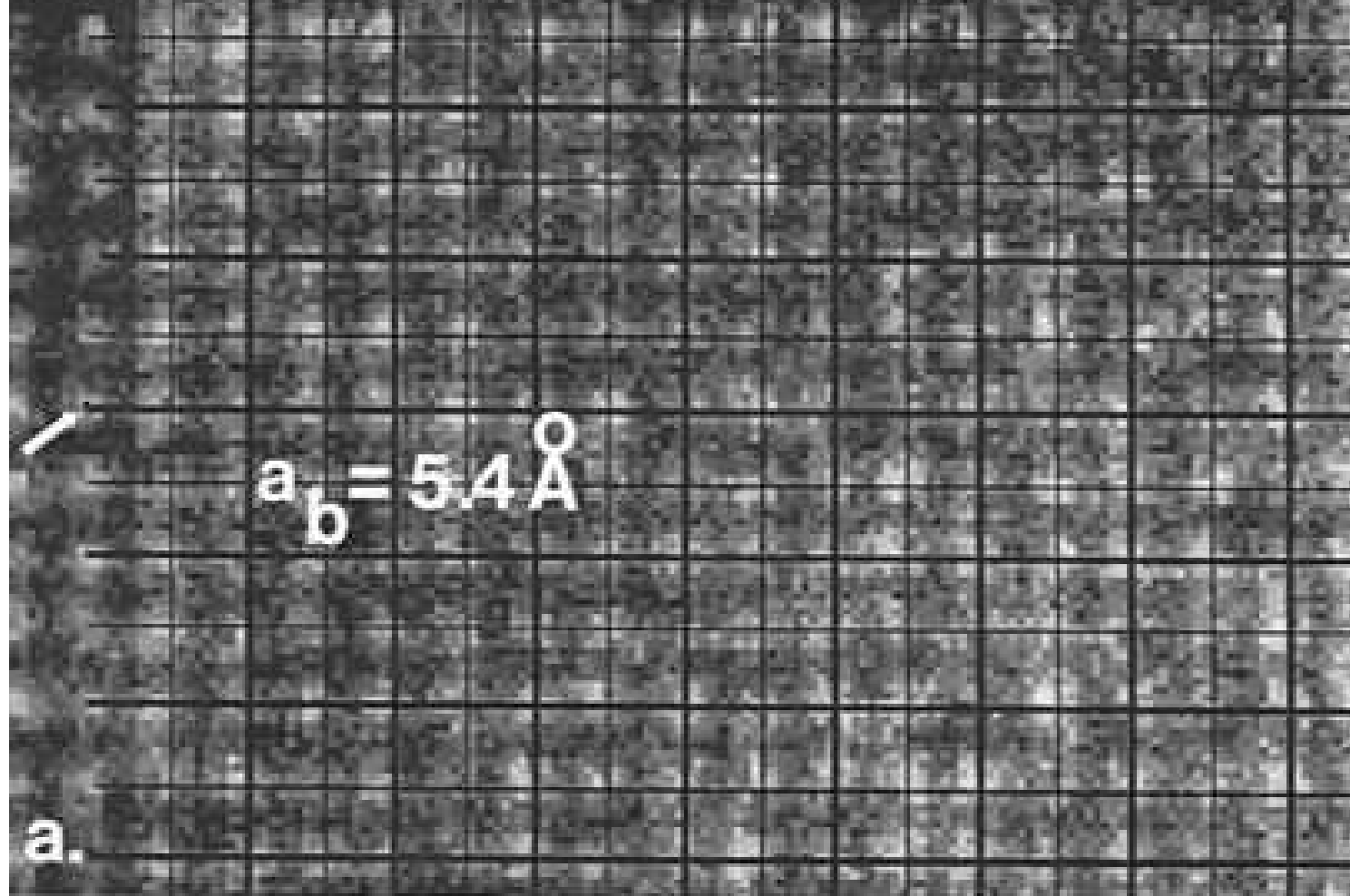
b) This is better seen in this, doubly filtered, high magnified detail of Fig.3b. White arrows left are added as the position control mark

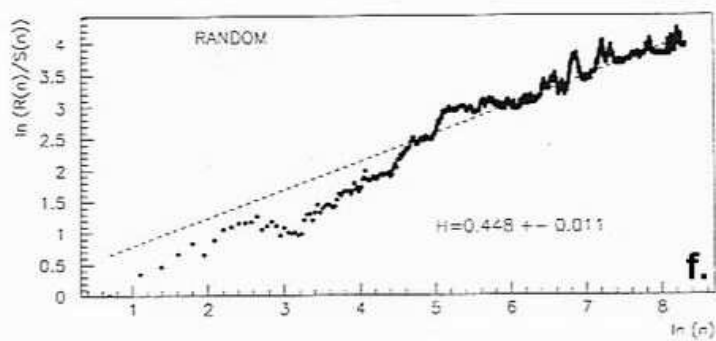
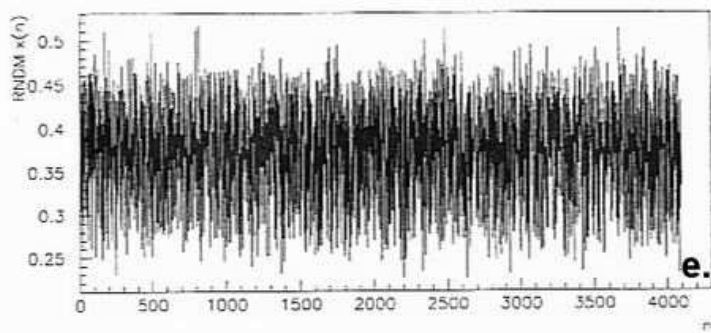
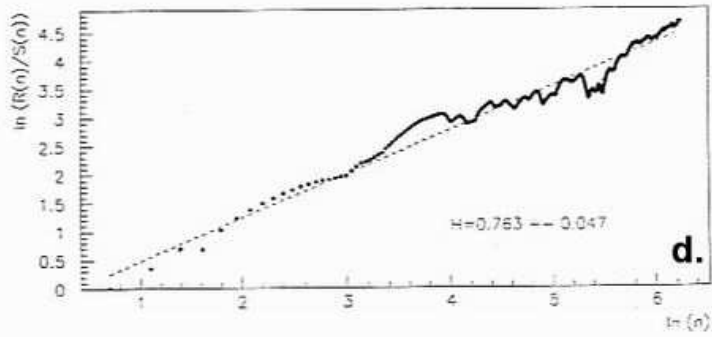
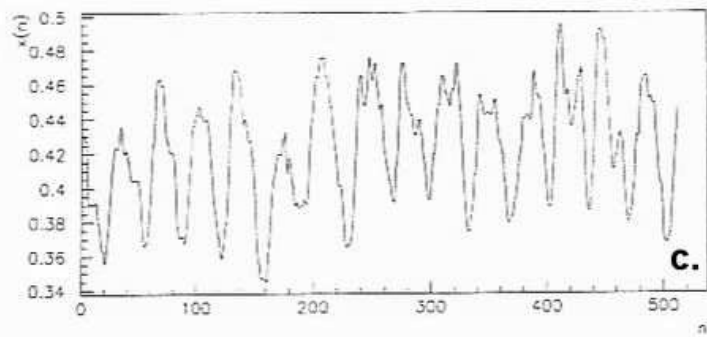
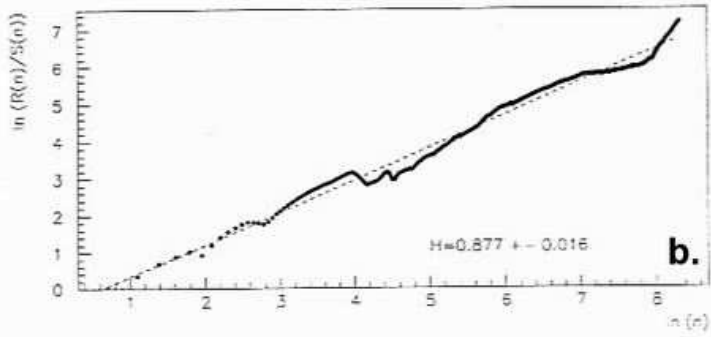
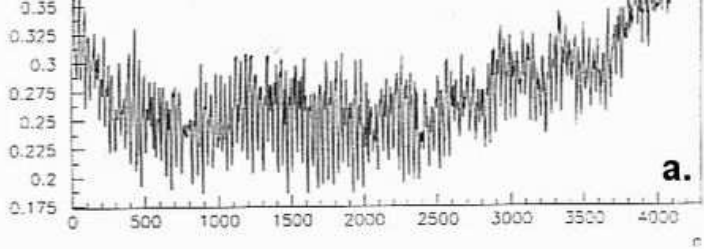
- Fig.5 a) The trace along [200] direction, containing 4096 measured points of the densitogram, the part of which is shown in Fig.2a. Similar traces are obtained for all measurements analyzed in the present paper.
- b) The R/S analysis of the trace in a).
- c) The "512 points" trace.
- d) The R/S analysis of the trace in c).
- e) Randomized "4096" trace.
- f) The R/S analysis of randomized trace in e), showing no ordering (H close to 0.5.).
- Fig.6 a) The ProFFT analysis of diffusely scattered electrons in the 1st and 2nd B.z. in the [100] direction. Absorption and re-emission regular bands of inelastically scattered electrons can be easily recognized.
- b) The same argumentation holds for [010]. Dark and white bands are nearly equidistant and of the order of atom spacings in the crystal.
- Fig.7 a) Combined figure, containing the effects of the diffuse diffraction in 1st and 2nd B.z., in the [100] and the [010] directions. See the details in the text.
- b) As in a), but with the "narrow cross". Similarities in both figures point to the Chaotic behaviour of the inelastically scattered electrons, as discussed in the text.
- Fig.8 a) The situation for the Fermi acceleration model. b) Quantum mechanical wave function for a quantum billiard system. c) The ProFFT analysis of Fig.1a using the "selection" ring for the electrons of nearly equal total energy loss, near the edge of the 1st Brillouin zone. The ring takes electrons diffracted in all directions with the energy loss so they point to the edge of the 1st Brillouin zone. The similarity with b) is obvious.





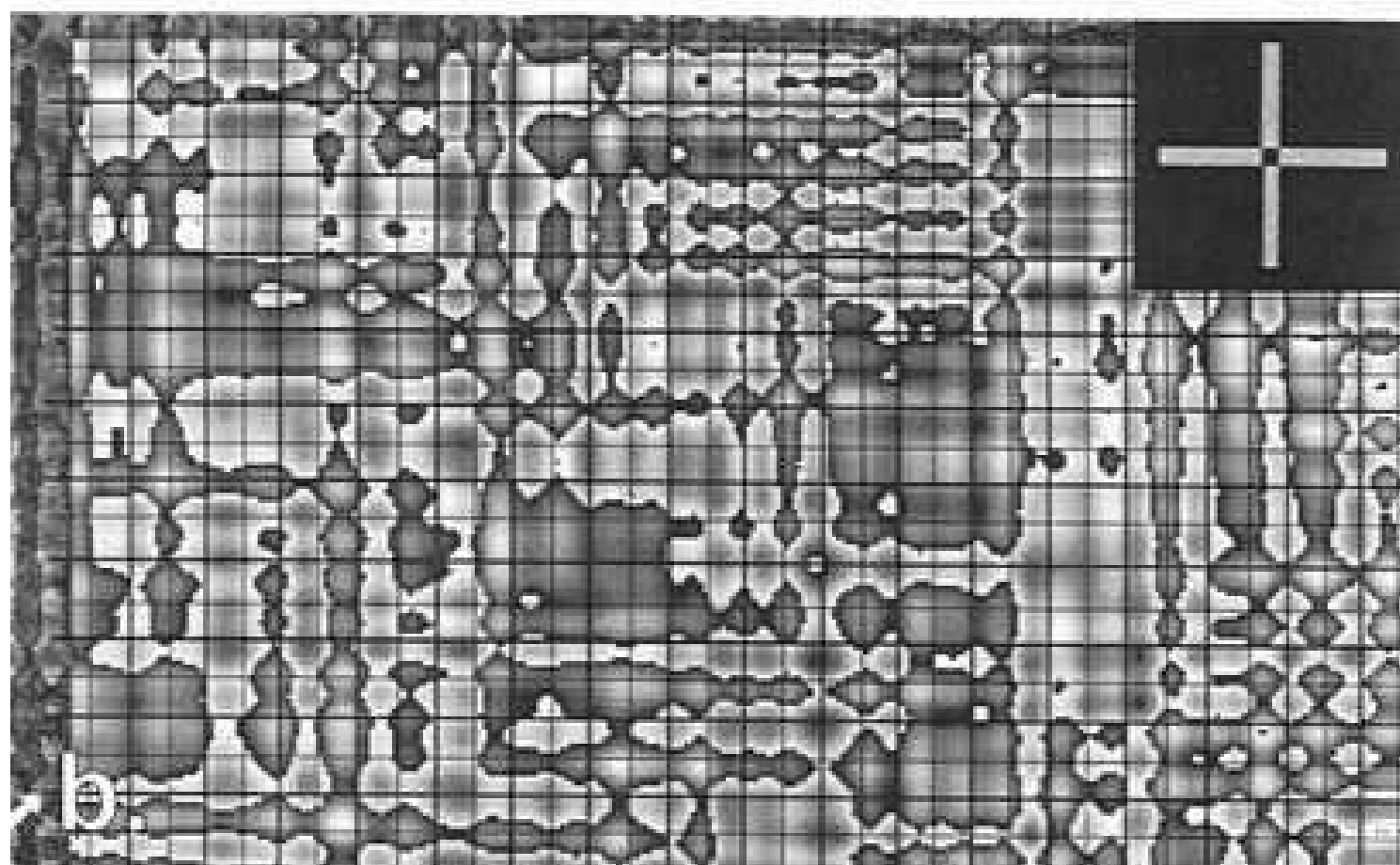
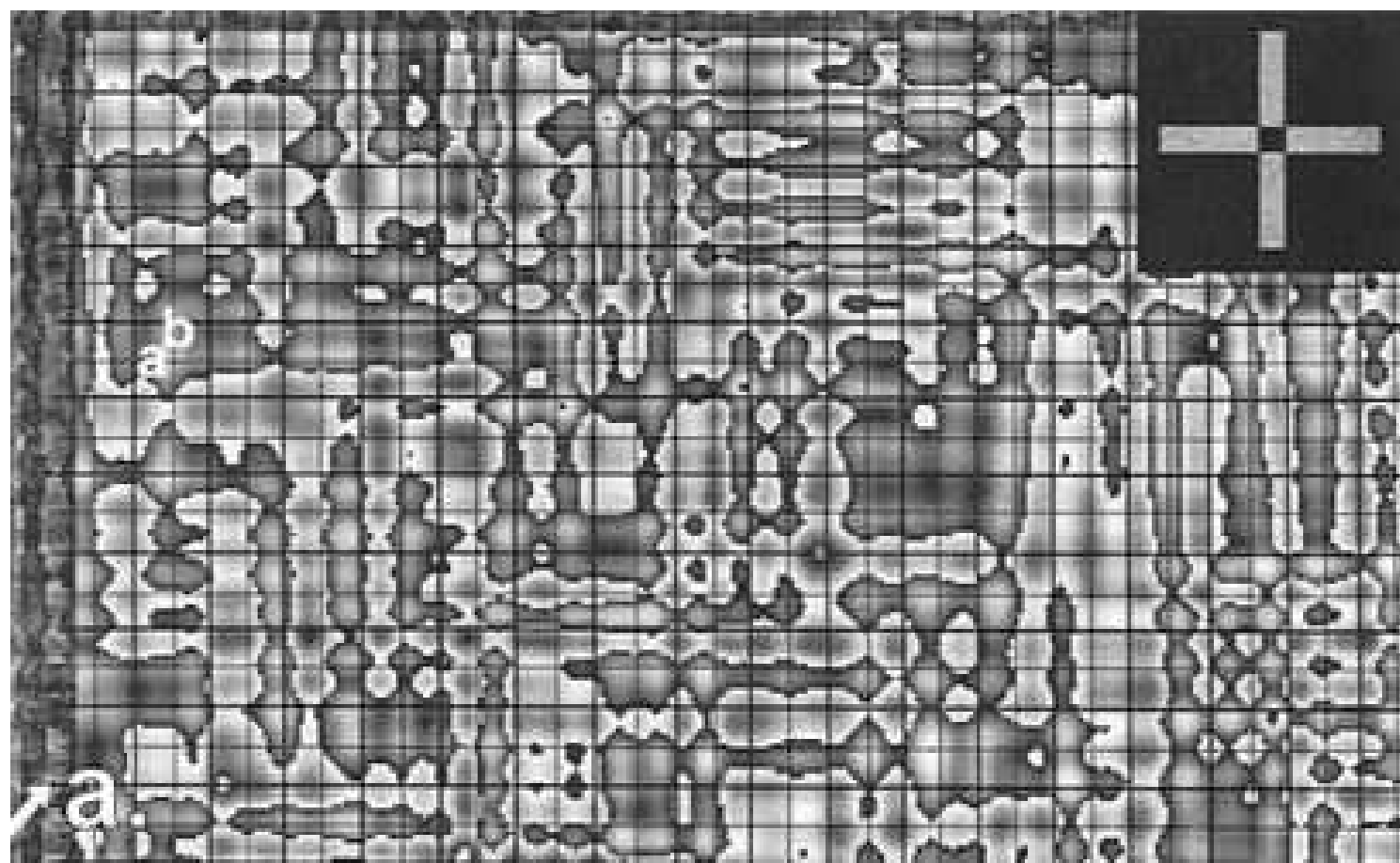


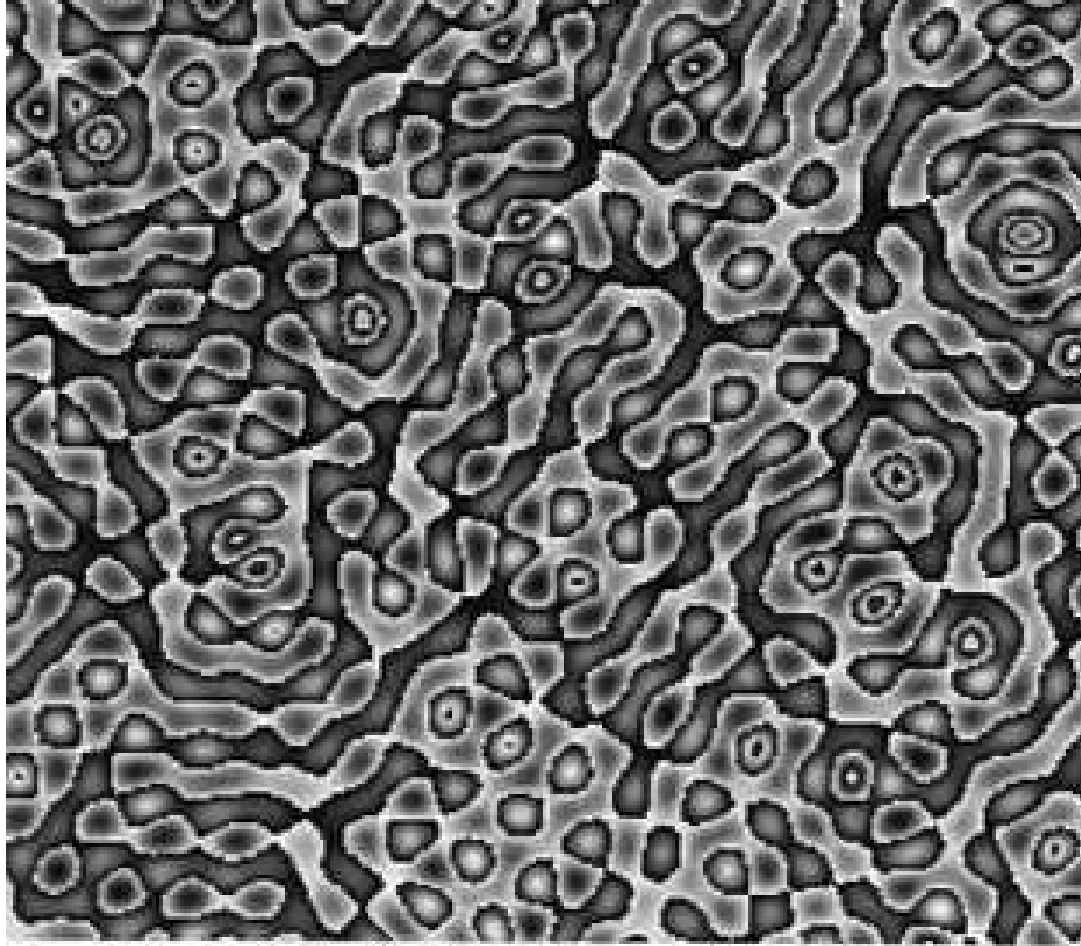




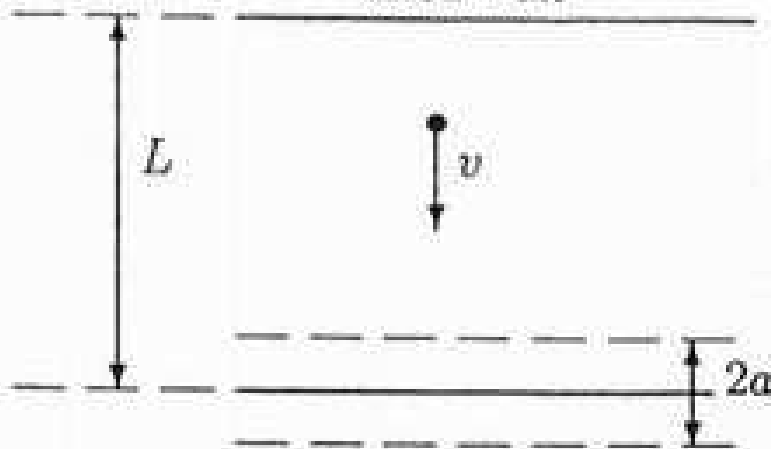
a.

b.





fixed wall



oscillating wall

